An Experimental Study on the Radiation Noise Characteristics of a Centrifugal Pump with Various Working Conditions

Chang Guo [1], Ming Gao [1,*] [ID], Dongyue Lu [2] and Kun Wang [1]

[1] School of Energy and Power Engineering, Shandong University, Jinan 250061, China; gg3263@163.com (C.G.); sduwang1993@163.com (K.W.)

[2] State Nuclear Power Engineering Company, Shanghai 200233, China; ldy11energy@163.com

* Correspondence: gm@sdu.edu.cn; Tel.: +86-531-8839-9008

Abstract: To investigate the radiation noise characteristics of a centrifugal pump under various working conditions, a noise measurement system is established; afterwards, the distribution of different points and intervals, as well as the overall level of noise, are studied. The total sound pressure level distribution for different points manifests the dipole and asymmetric directivity characteristics. Additionally, the acoustic energy is introduced to compare the noise of different intervals to reveal the asymmetric characteristics, and it is found that variation in working conditions has little impact on the acoustic energy distribution, and the ratio of the acoustic energy in the direction facing the tongue, as well as that in the direction against the tongue, to total acoustic energy fluctuate around 0.410 and 0.160, respectively, under various working conditions. Also, the A-weighted average sound pressure level (L_{pA}) is applied to describe the overall level of noise, and L_{pA} increases gradually with the growth of rotational speed, but the growth slope decreases. While in the operation of throttling regulation, L_{pA} shows the trend that first increases, then remains stable, and increases again with the growth of flow rate. This study could provide guidance for optimizing the operating conditions and noise control of centrifugal pumps.

Keywords: centrifugal pump; radiation noise; distribution characteristic; acoustic energy; experimental research

1. Introduction

Widespread concerns about environmental protection are accelerating noise abatement investment, accounting for 15–20% of the environmental protection investment [1]. Centrifugal pumps, widely applied in many fields of national economy [2,3], radiate a lot of noise during operation. The unexpected noise could affect the flow performance and deteriorate the working environment. To establish theoretical basis of radiation noise control technology for centrifugal pumps, this study reveals the changing rules of radiation noise under various working conditions.

Experimental studies could provide the most reliable results for scholars to detect the noise from centrifugal pumps. Choi et al. [4] conducted experiments and revealed that the main cause of radiation noise generated by an impeller without volute was the pressure fluctuation on the blade surface. Chu et al. [5,6] took the volute into consideration and attributed the primary noise to the interaction between the non-uniform outflux from the impeller and tongue [5,6], and further research showed that a slight increase of the gap between impeller and tongue would reduce the noise significantly [7]. Parrondo et al. [8] established an acoustic model to characterize the internal sound field at low frequency range, and concluded that the internal sound field could be characterized by a dipole-like source near the tongue. Cai et al. [9] measured the pressure fluctuation near the wall of the

tongue under various rotational speed conditions, and found that the pressure fluctuation intensity increased more rapidly than that of rotational speed. The four-port model was introduced for research on internal sound fields in pipes, making it convenient to change the rules of noise in pipes under various working conditions [10–12]. Based on LabVIEW (LabVIEW8.6, National Instruments, Austin, Texas, USA), Yuan et al. [13] designed a measurement system for internal noise analysis of centrifugal pumps with synchronous measurement for noise signal, pressure and flow rate, and laid a foundation for the follow-up study about the influence of different structures [14–16] on sound pressure levels (SPL) at different frequencies. To characterize far field radiation noise, Ye et al. [17] measured the noise amplitude outside a centrifugal pump under various flow rate conditions, and found that noise amplitude reached maximum at the highest efficiency point.

Currently, as a useful research tool, numerical simulation compensated for weaknesses in the experiment. A hybrid method combining computational fluid dynamics (CFD) with Lighthill acoustic analogy was widely used to elucidate the acoustic generation [18,19]. Langthjem and Olhoff [20,21] applied the hybrid method for noise calculation in a two-dimensional centrifugal pump, and concluded that the main cause of noise was the dipole source. The dipole source was defined as unsteady fluid force acting on the wall surface, including the impeller and volute source, in centrifugal pumps. Huang et al. [22], Ma et al. [23] and Liu et al. [24] considered the two dipole sources to be the noise source for acoustic calculation, and compared the SPL at different orders of blade passing frequency (BPF) with different structures, and this research provided guidance for structural optimization of centrifugal pumps. In addition, Gao et al. [25] discovered that the radiation noise generated by an impeller demonstrated diploe directivity, while the volute-generated noise appeared to have asymmetric directivity, i.e., the noise level in the direction facing the tongue was higher than that of the direction against the tongue. Dong et al. [26] pointed out that the volute-generated noise increased monotonously and nonlinearly with the increase of rotational speed.

Obviously, the literature shows that previous experimental research mainly focused on the internal noise characteristics in pipes, while merely experimental research focused on far field radiation noise. During the numerical simulation, the previous research mainly considered the influence of the impeller dipole source and volute dipole source on the radiation noise separately, and most are the SPL at different orders of BPF. Actually, the radiation noise results from the interaction of the two dipole sources when pumps are running, so the interaction influence should be considered to obtain more accurate results. In addition, it is necessary to calculate the total sound pressure level (TSPL) of different monitoring points, calculated by the superposition of SPL at different characteristic frequencies, to acquire the directivity characteristic. Noise propagation is the spread of acoustic energy in the medium, so the acoustic energy changes with noise propagation process and the directivity characteristic can be detected. The overall level of radiation noise should also be conducted to evaluate the noise intensity under specific working conditions. In general, the pumps are always working at various conditions with various working demands, and the radiation noise changes accordingly, and it is also indispensable to carry out the various working condition study for radiation noise to figure out these changing rules.

In this paper, a centrifugal pump radiation noise measurement system is established. Then, the TSPL and acoustic energy distribution, as well as the overall level of radiation noise, are analyzed, which may provide guidance for optimizing the working conditions and noise control of centrifugal pumps.

2. Experimental Facility and Procedure

2.1. Parameters of the Test Pump

In this study, IS-80-50-250 (IS-80-50-250, Shanghai Pump Manufacture Co., Ltd, Shanghai, China) is chosen as the test pump, and the prototype figure is shown in Figure 1. Water at normal temperature is used as medium, and the geometric and performance parameters of the test pump are listed in Table 1.

Figure 1. Prototype figure of the test pump.

Table 1. Geometric and performance parameters of the test pump.

Parameter	Value
Inlet diameter, mm	80
Impeller diameter, mm	250
Outlet diameter, mm	50
Nominal flow rate, m^3/h	50
Best efficiency	63% (50 m^3/h)
Design head, m	80
Nominal rotational speed, rpm	2900
Blade number	6

2.2. Radiation Noise Measurement System

The experimental apparatuses used in the system are shown schematically in Figure 2, which include a soundproof room, water circulation system, circuit control system, and data acquisition and storage system. In the measurement system, to reduce the influence of the surrounding environment and motor operation on the measurement results, the centrifugal pump and motor are insulated by a soundproof room; the interior and exterior walls of the soundproof room, along with the motor, are surrounded by soundproof cotton. The pump is driven by the YVF2180L-2 type three-phase asynchronous motor (YVF2180L-2, Shanghai Nama Electric Co., Ltd, Shanghai, China), and the rotational speed is regulated by the Y0300G3 type frequency converter (Y0300G3, Shanghai Nama Electric Co., Ltd, Shanghai, China). The flow rate, inlet pressure, outlet pressure, as well as the radiation noise level are measured and recorded by corresponding instrument listed in Table 2.

During the operation, when the operation system reaches stable, the flow rate, pressure, radiation noise level are measured sequentially and stored in the computer terminal. After that, the rotational speed and flow rate are adjusted via frequency converter and artificial regulation, respectively, then these parameters under various working conditions are recorded for analysis. Figure 3 shows the structure diagram of the measurement system.

Table 2. Measurement characteristic of instruments.

Instruments	Type	Application	Measuring Range	Accuracy or Sensitivity
Flow meter	SLDG-800 (SLDG-800, Nanjing Shunlaida Measurement and Control Equipment Co., Ltd., Nanjing, Jiangsu, China)	Measuring flow rate	0–100 m^3/h	0.2% (accuracy)
Pressure transducer	MIK-300 (MIK-300, Hangzhou Meikong Automation Technology Co., Ltd., Hangzhou, China)	Measuring inlet pressure	−100–0 kPa (inlet pipe)	0.5% (accuracy)
		Measuring outlet pressure	0–1600 kPa (outlet pipe)	0.5% (accuracy)
Pressure recorder	RX-200D (RX-200D, Hangzhou Meikong Automation Technology Co., Ltd., Hangzhou, China)	Recording pressure	/	/
Microphone	AWA14423L (AWA14423L, Hangzhou Aihua Instruments Co., Ltd., Hangzhou, China)	Measuring radiation noise	10–20 kHz	50 mV/Pa (sensitivity)
Two channel signal analyzer	AWA6290M+ (AWA6290M+, Hangzhou Aihua Instruments Co., Ltd, Hangzhou China)	Recording radiation noise	/	/
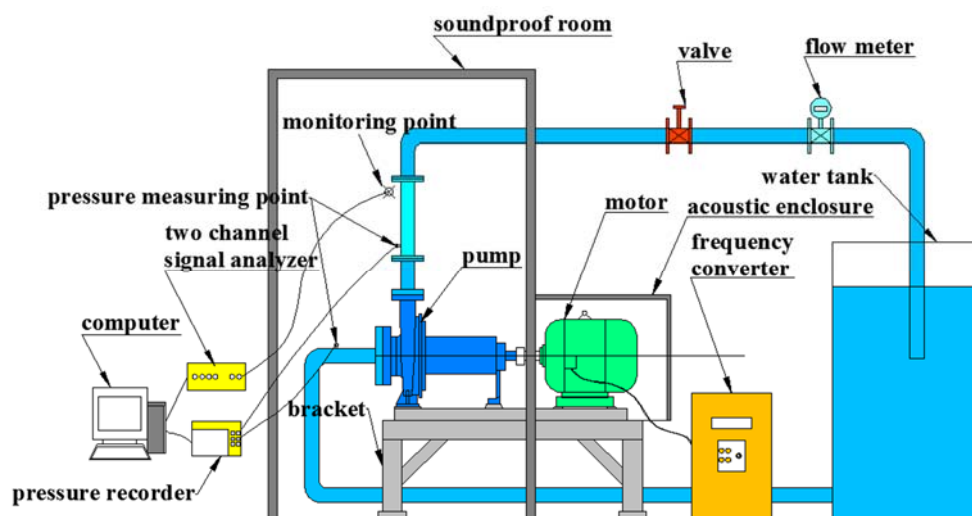
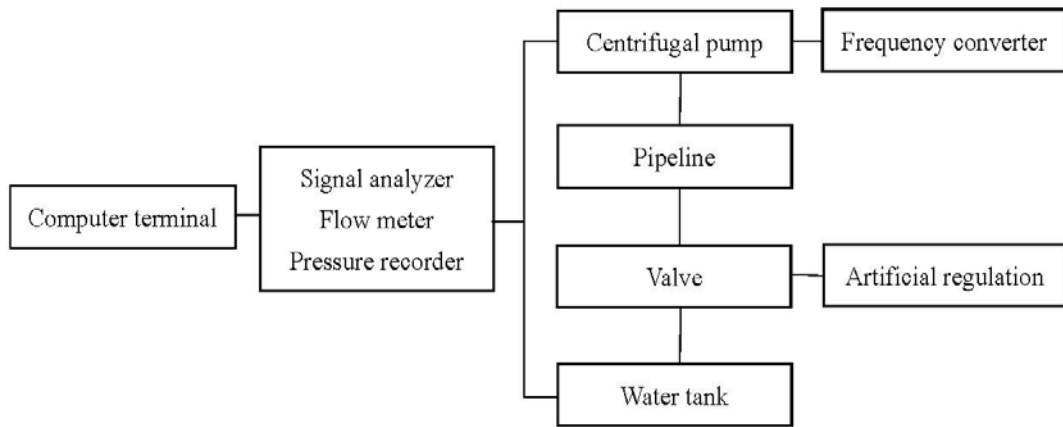**Figure 2.** Layout and instrumentation of measurement system.

Figure 3. Structure diagram of measurement system.

2.3. Arrangement of the Monitoring Points

To acquire the distribution characteristic of radiation noise, 16 monitoring points are arranged on the measurement surface around the pump. As shown in Figure 4, the monitoring points are 1000 mm away from the center of impeller, and arranged evenly in circumferential directions [27]. During the measurement process, SPL characteristic of every point is measured sequentially by a microphone. Here, SPL is defined as:

$$SPL = 20 \log \frac{P_e}{P_{ref}} \tag{1}$$

$$P_e = \sqrt{\frac{1}{T} \int_0^T p'^2 dt} \tag{2}$$

$$T = \frac{t}{l} \tag{3}$$

where P_{ref} is the reference acoustic pressure (2×10^{-5} Pa in air), P_e is the effective value of acoustic pressure, p' is instantaneous acoustic pressure, t is the time of one revolution of the impeller, and l is the number of blades ($l = 6$ in this paper).
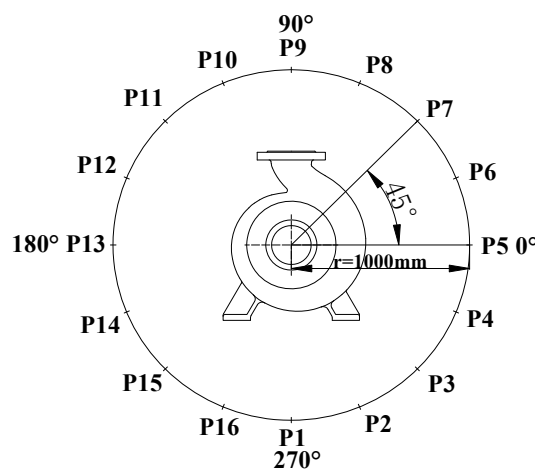

Figure 4. Arrangement of monitoring points in circumferential direction.

To reveal the noise intensity of different monitoring points and the directivity characteristic, it is necessary to derive a temporal intensity profile involving a superposition of SPL at each Fourier frequency. Thus TSPL is introduced and given by:

$$\text{TPSL} = 10\lg\sum_{i=1}^{n} 10^{\text{SPL}_i/10} \tag{4}$$

where n represents the number of frequencies. However, TSPL only represents the noise level of a certain monitoring point, and it can't be superimposed by arithmetic to describe the noise level of an interval. Therefore, the acoustic energy is more suitable for comparing the noise level of different monitoring intervals since it can be superimposed by arithmetic, moreover, the propagation of sound is essentially the propagation of energy. Briefly, the application of acoustic energy could reveal the noise level relationship between different intervals intuitively, so the average acoustic energy density [28] is analyzed, and it is defined as:

$$\varepsilon = \frac{P_e^2}{\rho c^2} \tag{5}$$

where ε, ρ and c represent the acoustic energy density, medium density (1.29 kg/m^3 in air) and the sound speed in medium (343 m/s in air), respectively.

To further evaluate the overall level of radiation noise on measurement surface, the average A-weighted sound pressure level (L_{pA}) of the measurement surface is introduced and expressed as:

$$L_{pA} = 10\lg\left(\frac{1}{m}\sum_{i=1}^{m} 10^{\text{TSPL}_i/10}\right) \tag{6}$$

where m represents the number of monitoring points, and the L_{pA} of 16 monitoring points on the measurement surface around the pump is calculated for analysis.

3. Radiation Noise Characteristic under Various Rotational Speed Conditions

The variable speed regulation has no throttling loss, and is an ideal adjustment method. In this section, on the basis of keeping the flow valve installed downstream on the outlet pipe opened fully and unchanged, then the radiation noise characteristic under various rotational speed conditions are studied. According to the similarity law, the relationship between flow rate and rotational speed is defined as:

$$\frac{Q_1}{Q_2} = \frac{n_1}{n_2} \tag{7}$$

where Q and n represent the flow rate and rotational speed, while the subscript 1 and 2 represent two different working conditions. It can be found that the flow rate is proportional to the rotational speed, so the flow rate of the centrifugal pump increases with the rise in rotational speed. To ensure the safety of the running system, seven different rotational speeds that are less than or equal to the nominal rotational speed are considered. The rotational speeds and corresponding flow rates are shown in Table 3.

Table 3. Rotational speeds and corresponding flow rates.

Rotational Speed, rpm	Flow Rate, m^3/h
1700	56.9
1900	64.8
2100	69.6
2300	74
2500	78.2
2700	82.1
2900	86

3.1. Directivity Characteristic of Radiation Noise under Various Rotational Speed Conditions

By measuring the SPL characteristic and calculating the TSPLs of 16 different points in the circumferential direction, the directivity of radiation noise is obtained under various rotational speed conditions.

As shown in Figure 5, it can be found that the TSPL increases from 80 to 100 dB with the increase of rotational speed. As a result of the symmetric characteristic of impeller, the directivity profile diagram of TSPL demonstrates the dipole symmetry, and one sees that the two TSPL valleys appear at 0° and 180°. In addition, apparent asymmetric characteristics also can be found due to the asymmetric structure of the volute, more concretely, the noise level in the direction facing the tongue (in the interval from 90° to 157.5°) is higher than that in the direction against the tongue (in the interval from 292.5° to 0°), which means that the radiation noise is the interaction result of impeller and volute dipole source.
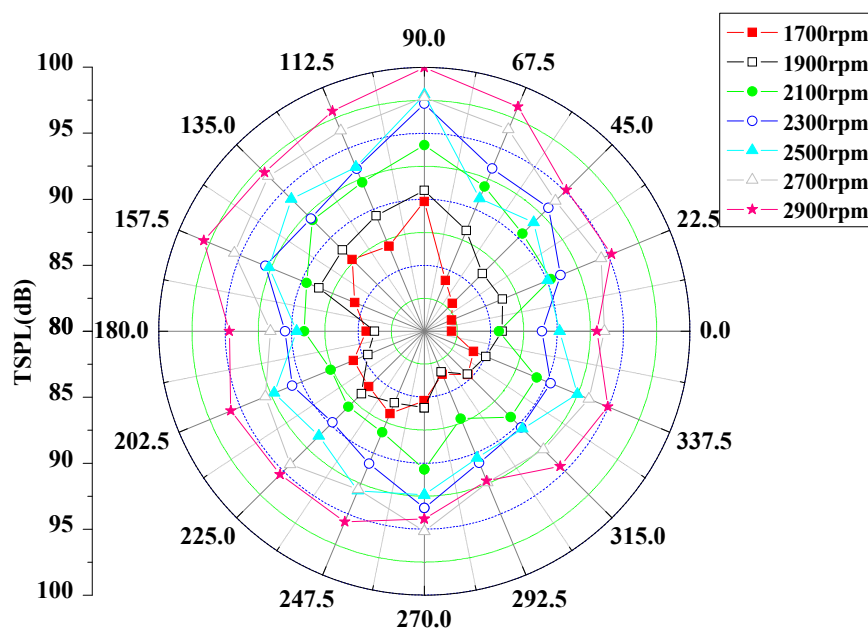

Figure 5. Directivity characteristic of radiation noise under various rotational speed conditions.

To further reveal the asymmetric characteristics under various rotational speed conditions quantitatively, the ratio of the acoustic energy in the interval from 90° to 157.5° (ε_1), as well as that in the interval from 292.5° to 0° (ε_2) to the total acoustic energy (ε_t) are calculated. As shown in Figure 6, the values of $\varepsilon_1/\varepsilon_t$ and $\varepsilon_2/\varepsilon_t$ change little with the change of rotational speed, and the value of $\varepsilon_1/\varepsilon_t$ fluctuates around 0.413, while the value of $\varepsilon_2/\varepsilon_t$ fluctuates near 0.157. This proves that the change of rotational speed would affect the acoustic energy, but it has little impact on the acoustic energy distribution. According to the past research [5–7], the volute tongue is the major noise source, and the measurement interval in the direction facing the tongue is closer to the tongue than other intervals. On the other hand, acoustic energy weakens gradually as the distance from the sound source increases, so the acoustic energy has less attenuation in the direction facing the tongue than that in the direction against the tongue, causing a much higher ratio of acoustic energy in the direction facing the tongue.
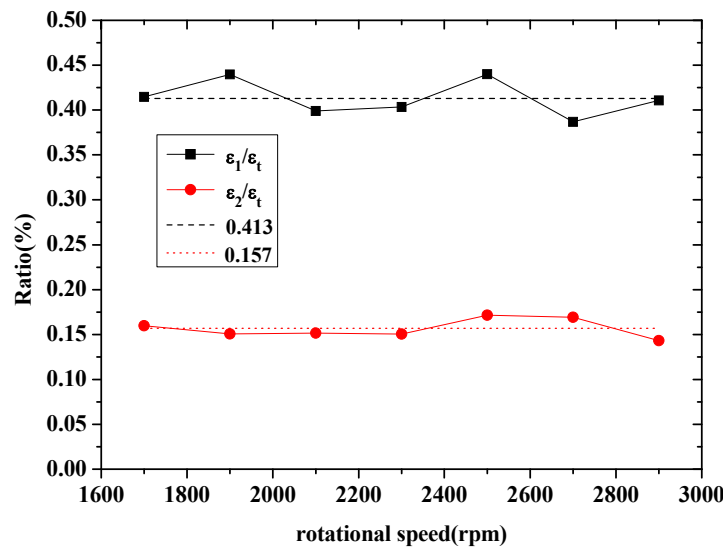
Figure 6. The acoustic energy changing curves with rotational speed.

3.2. Changing Rules of Radiation Noise under Various Rotational Speed Conditions

To analyze the noise level changing rules of different points under various rotational speed conditions, P1 (270°, in the direction against the outlet), P5 (0°, the valley point), P9 (90°, in the direction facing the outlet), P11 (135°, in the direction facing the tongue) and P13 (180°, the valley point) are selected. As shown in Figure 7, it can be more visually seen that the TSPLs of different monitoring points rise with the rotational speed increasing. In general, the TSPLs of P5 and P13 are lower than the others because the two points are located at the valley of dipole characteristic, meanwhile, TSPL of P1 lies between P5 and P11. As a result of the influence of volute tongue noise source, P9 and P11 have a higher noise level, and P9 is located in outlet direction, which is more affected by the internal flow noise in outlet pipe, so P9 is the highest noise level point.
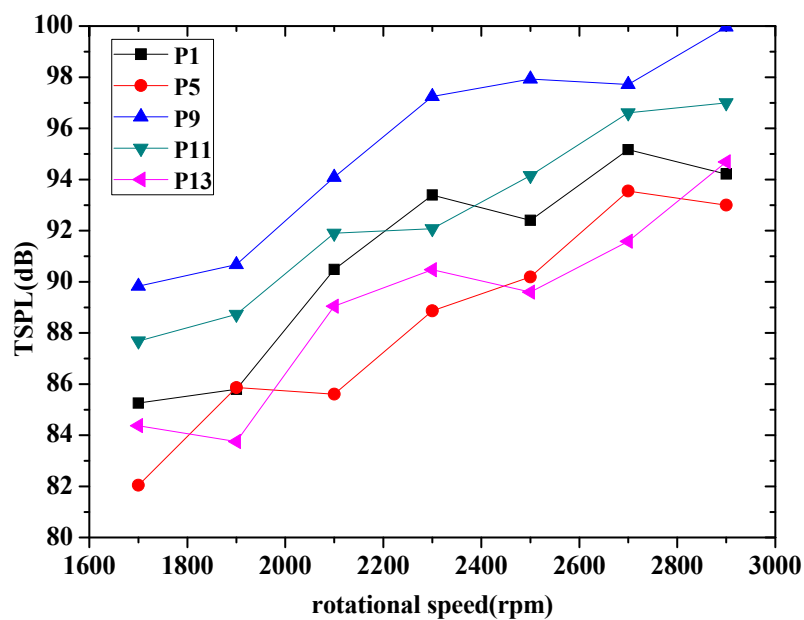

Figure 7. TSPL changing curves with rotational speed.

To evaluate the overall level of radiation noise, the L_{pA} of the 16 monitoring points is compared in Figure 8 under various rotational speed conditions. It can be observed that L_{pA} climbs gradually with the increase of rotational speed, and reaches to maximum at 2900 rpm. When rotational speed increases from 1700 to 2900 rpm, the L_{pA} increases by 12.40%. However, the growth slope decreases gradually with the increase of rotational speed generally, in particular, the L_{pA} grows rapidly in the interval between 1700 and 2300 rpm, with an average increase of 1.12 dB per 100 rpm, while in the range from 2300 to 2900 rpm, the growth rate of L_{pA} slows down, with an average increase of 0.65 dB per 100 rpm, which is less than that in the range from 1700 to 2300 rpm. It could be explained by that with the increase of rotational speed, the pressure fluctuation on wall surface also increases, but the increment rate of the variance of pressure fluctuation decreases [29], and causes a slow increase in acoustic pressure around the pump, and as a result, the growth slope of noise level decreases steadily.
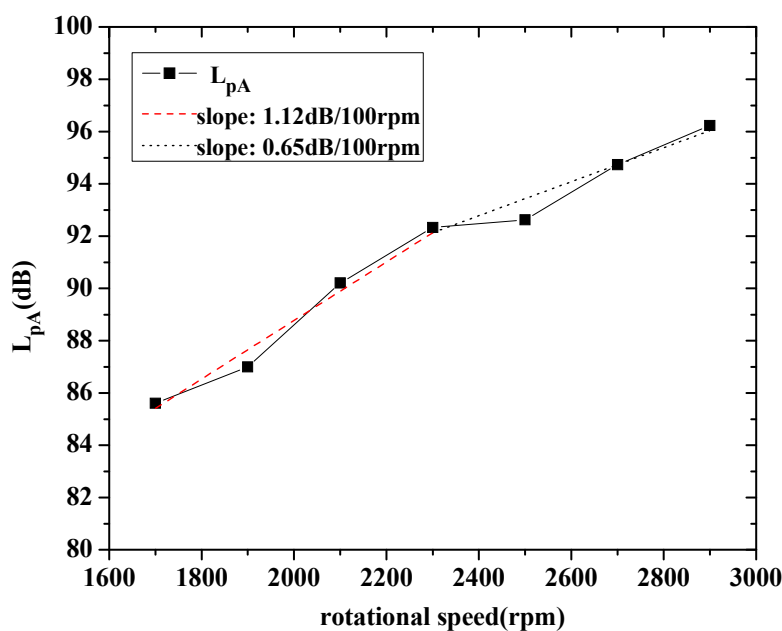

Figure 8. L_{pA} changing curve with rotational speed.

4. Radiation Noise Characteristics under Various Flow Rate Conditions

Compared with the variable speed regulation, the throttling regulation has the advantages of easy operation and low cost. Considering the two factors mentioned, throttling regulation is widely adopted at some occasions. In this section, the throttling regulation is realized by adjusting the valve opening on outlet pipe, then five different flow rates, i.e., 37.5, 50 (nominal flow rate), 62.5, 75 and 86 m^3/h (valve open fully), are studied to explore the radiation noise characteristic under various flow rate conditions when rotational speed is set as 2900 rpm.

4.1. Directivity Characteristic of Radiation Noise under Various Flow Rate Conditions

By calculating the TSPLs of 16 different points in the circumferential direction, then the directivity characteristic of radiation noise is analyzed under various flow rate conditions.

It is apparent in Figure 9 that TSPL changes between 86 dB and 100 dB, not only the dipole characteristic, but the asymmetric characteristic are presented in circumferential direction. And then the ratio of the acoustic energy in the interval from 90° to 157.5° (ε_1), as well as that in the interval from 292.5° to 0° (ε_2) to the total acoustic energy (ε_t) are compared under various flow rate conditions. As shown in Figure 10, the values of $\varepsilon_1/\varepsilon_t$ and $\varepsilon_2/\varepsilon_t$ show the fluctuation trend in the vicinity of 0.410 and 0.166, respectively. And these results are closer to those under various rotational speed conditions. It also can be found that the deviation between the value of $\varepsilon_1/\varepsilon_t$ and average value (0.410) is larger

at 50 m^3/h. It could be explained by that in the measurement process, the measurement results are affected by the severe disturbance of the surrounding environment, but it does not affect the conclusion that the change of flow rate also has little impact on the acoustic energy distribution.
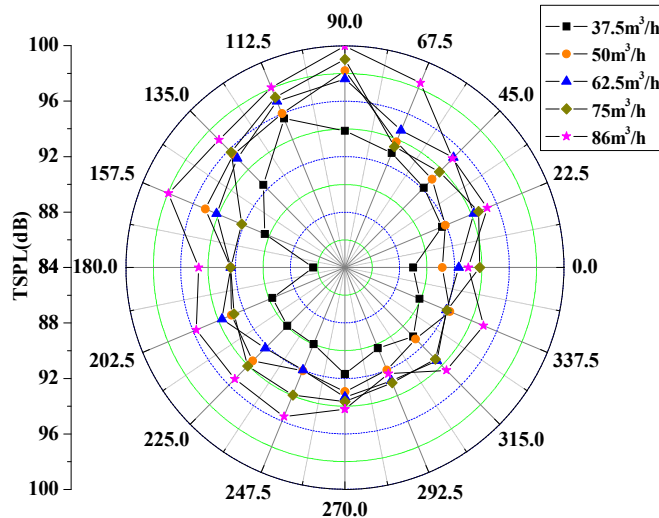

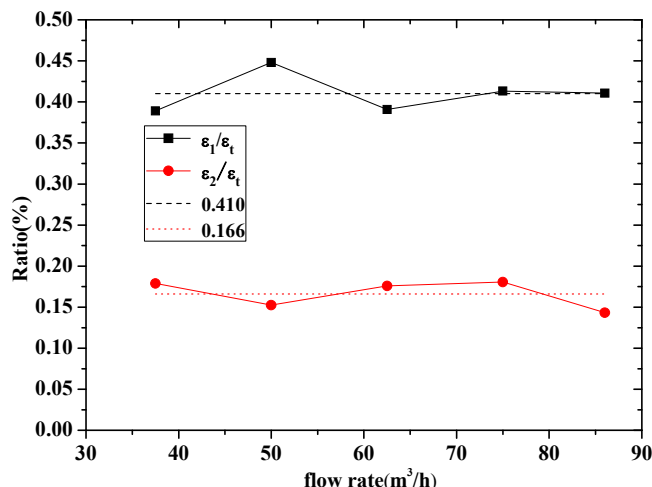**Figure 9.** Directivity characteristics of radiation noise under various flow rate conditions (2900 rpm).

Figure 10. The acoustic energy changing curves with flow rate (2900 rpm).

4.2. Changing Rules of Radiation Noise under Various Flow Rate Conditions

In Figure 11, TSPLs of P1, P5, P9, P11 and P13 are also analyzed to reveal the noise level changing rules under various flow rate conditions. It is revealed that TSPLs of different points show similarly changing rules, specifically, the TSPL increases rapidly in small flow range from 37.5 to 50 m^3/h, then basically levels off in the interval from 50 to 75 m^3/h, and continues to increase when flow rate is higher than 75 m^3/h. What's more, the TSPL distribution characteristic of different points under various flow rate conditions also shows that the noise level at P5 and P13 are lower than others, while TSPLs of P9 and P11 are higher than others, and P9 is highest noise level point, which coincides with the distribution under various rotational speed conditions.
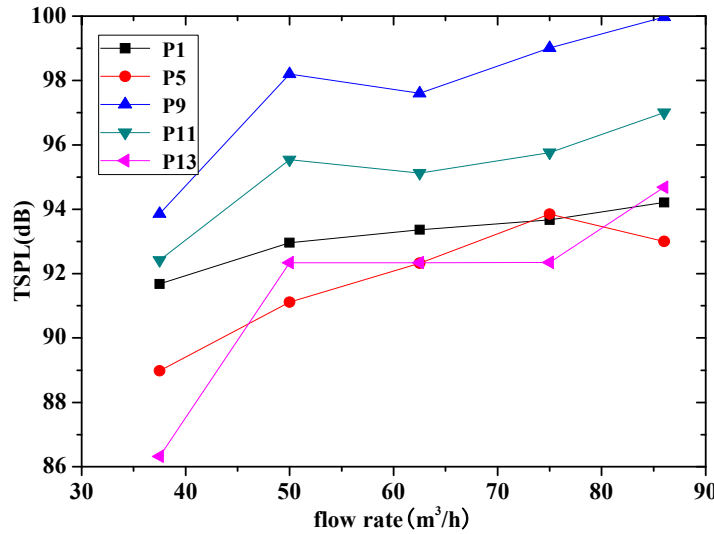
Figure 11. TSPL changing curves with flow rate (2900 rpm).

Furthermore, L_{pA} of 16 monitoring points is also studied under various flow rate conditions. It can be found in Figure 12 that the L_{pA} also increases sharply initially at small flow rate, then maintains stable, and reaches to maximum value at large flow rate interval. Additionally, L_{pA} changes a little with the increase of flow rate, which increases by 5.10% when flow rate grows from 37.5 to 86 m^3/h.
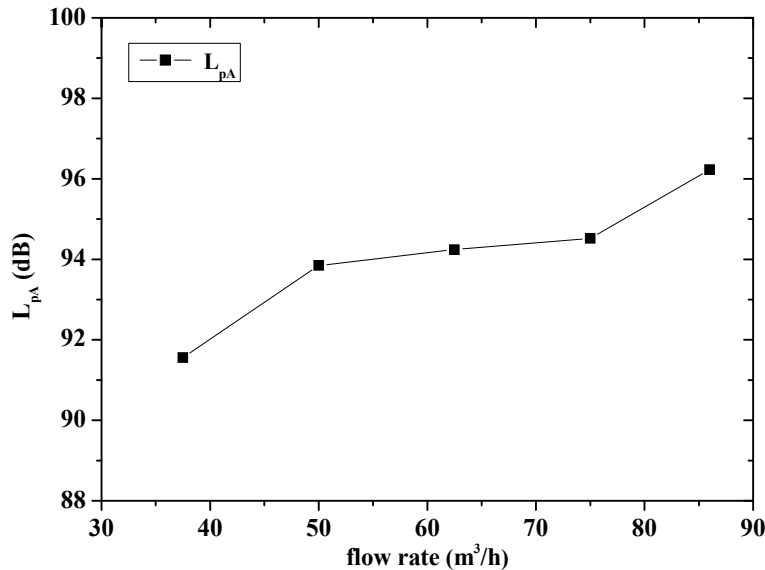

Figure 12. L_{pA} changing curve with flow rate (2900 rpm).

To explore the reasons for the changing rules of L_{pA} under various flow rate conditions, the head and efficiency are calculated, respectively. The changing rules of the two parameters are shown in Figure 13, it can be found that with the increase of flow rate, the head decreases gradually. In addition, the efficiency shows the tendency that increases from 37.5 to 50 m^3/h, and reaches to the maximum at 50 m^3/h, then remains essentially unchanged in the range from 50 to 75 m^3/h, which is the best efficiency range, and it keeps decreasing subsequently with the flow rate continues to grow. At low flow rate conditions, the pressure fluctuation inside the pump is low and causes low noise levels. With the increase of flow rate, the pressure fluctuation inside the pump increases accordingly, while in the best efficiency range, i.e., in the range from 50 to 75 m^3/h, the pressure becomes stable [17],

and leads to little change for the noise level. However, as the flow rate continues to increase, the head and efficiency decrease dramatically, which may be caused by the occurrence of cavitation inside the pump, and contribute to the dramatic increase of L_{pA} when flow rate is greater than 75 m^3/h.
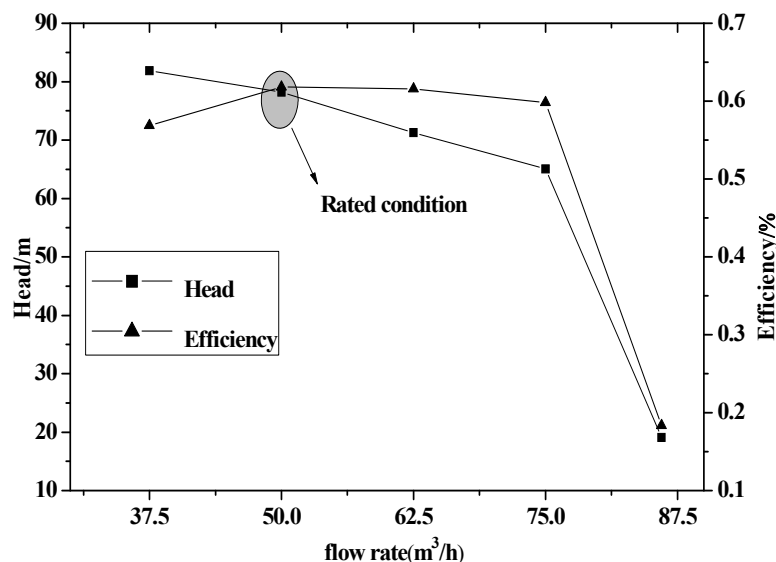

Figure 13. Head and efficiency changing curve with flow rate (2900 rpm).

5. Conclusions

In this paper, a centrifugal pump radiation noise measurement system is established, then the directivity distribution characteristics and overall level of radiation noise are analyzed under various working conditions. The main conclusions are drawn as follows:

(a) Under various working conditions, the total sound pressure level distribution for different monitoring points is dipolar; specifically, the two valley values appear at 0° (in the direction against the tongue) and 180°, and the minimum valley values are presented at the minimum rotational speed and minimum flow rate condition. Additionally, asymmetry is also validated, i.e., the noise level in the direction facing the volute tongue is higher than that in the direction against the tongue, and the monitoring point in outlet direction is the highest noise level point.

(b) The change in working conditions has little impact on the acoustic energy distribution of different intervals, and the ratios of the acoustic energy in the direction facing the tongue (ε_1), as well as that in the direction against the tongue (ε_2), to the total acoustic energy (ε_t) fluctuate around 0.410 and 0.160, respectively.

(c) In the operation of variable speed regulation, the average A-weighted sound pressure level (L_{pA}) increases gradually with the increasing of rotational speed, and it increases by 12.40% when rotational speed increases from 1700 to 2900 rpm, but the growth slope decreases gradually with the rise of pump rotational speed. While in the operation of throttling regulation, L_{pA} first increases, then remains stable, and continues to increase with the increase in flow rate, and it increases by 5.10% when flow rate grows from 37.5 to 86 m^3/h.

Author Contributions: Chang Guo, Dongyue Lu designed the study, conducted the experiment and collected the experimental data; Kun Wang analyzed the experimental data; Chang Guo wrote the manuscript; Ming Gao reviewed and edited the manuscript.

Conflicts of Interest: The authors declare no conflict of interest.

References

1. Mao, D.X.; Hong, Z.H. *Environmental Noise Control Engineering*; Higher Education Press: Beijing, China, 2002.
2. Shah, S.R.; Jain, S.V.; Patel, R.N.; Lakhera, V.J. CFD for centrifugal pumps: A review of the state-of-the-art. *Procedia Eng.* **2013**, *51*, 715–720. [CrossRef]
3. Wu, D.F.; Liu, Y.S.; Li, D.L.; Zhao, X.F.; Li, C. Effect of materials on the noise of a water hydraulic pump used in submersible. *Ocean Eng.* **2017**, *131*, 107–113. [CrossRef]
4. Choi, J.S.; Mclaughlin, D.K.; Thompson, D.E. Experiments on the unsteady flow field and noise generation in a centrifugal pump impeller. *J. Sound Vib.* **2003**, *263*, 493–514. [CrossRef]
5. Chu, S.; Dong, R.; Katz, J. Relationship between unsteady flow, pressure fluctuation, and noise in a centrifugal pump—Part A: Use of PDV data to compute the pressure field. *J. Fluid Eng.* **1995**, *117*, 24–29. [CrossRef]
6. Chu, S.; Dong, R.; Katz, J. Relationship between unsteady flow, pressure fluctuation, and noise in a centrifugal pump—Part B: Effects of blade-tongue interactions. *J. Fluid Eng.* **1995**, *117*, 30–35. [CrossRef]
7. Dong, R.; Chu, S.; Katz, J. Effect of Modification to Tongue and Impeller Geometry on Unsteady Flow, Pressure Fluctuations, and Noise in a Centrifugal Pump. *J. Turbomach.* **1997**, *119*, 506–515. [CrossRef]
8. Parrondo, J.; Pérez, J.; Barrio, R.; González, J. A simple acoustic model to characterize the internal low frequency sound field in centrifugal pumps. *Appl. Acoust.* **2011**, *72*, 59–64. [CrossRef]
9. Cai, J.C.; Pan, J.; Andrew, G. Experimental study of the pressure fluctuation around the volute tongue of a centrifugal pump at variable rotating speed. *Fluid Mach.* **2015**, *43*, 13–16.
10. Rzentkowski, G.; Zbroja, S. Experimental characterization of centrifugal pumps as an acoustic source at the blade-passing frequency. *J. Fluid Struct.* **2000**, *14*, 529–558. [CrossRef]
11. Wang, Q.Y. Numerical and Experimental Research on the Flow-Induced Noise of Centrifugal Pump in the Seawater Pipe. Master's Thesis, Harbin Engineering University, Harbin, China, 2010.
12. Si, Q.R.; Yuan, S.Q.; Yuan, J.P. Experimental study on the influence of impeller-tongue gap on the performance and flow-induced noise characteristics of centrifugal pumps. *J. Vib. Shock* **2016**, *35*, 164–168.
13. Yuan, S.Q.; Yang, Y.; Yuan, J.P.; Luo, Y. Measurement system design of flow-induced noise in centrifugal pumps. *Drain. Irrig. Mach.* **2009**, *27*, 10–14.
14. Liu, H.L.; Wang, Y.; Yuan, S.Q.; Tan, M.G. Effects of impeller outlet width on the vibration and noise from centrifugal pumps induced by flow. *J. Huazhong Univ. Sci. Technol.* **2012**, *40*, 123–127.
15. Tan, M.G.; Wang, Y.; Liu, H.L.; Wu, X.F.; Wang, W. Effects of number of blades on flow induced noise vibration and noise of centrifugal pumps. *J. Drain. Irrig. Mach. Eng.* **2012**, *30*, 131–135.
16. Wang, Y.; Liu, H.L.; Liu, D.X.; Wang, J.; Wu, X.F. Effects of vane wrap angle on flow induced vibration and noise of centrifugal pumps. *Trans. Chin. Soc. Agric. Eng.* **2013**, *29*, 72–77.
17. Ye, X.M.; Pei, J.J.; Li, C.X.; Liu, Z. Experimental Study on Nosie Characteristics of Centrifugal Pump Based on Near-Field Acoustic Pressure Method. *Chin. J. Power Eng.* **2013**, *33*, 375–380.
18. Wang, M.; Freund, J.B.; Lele, S.K. Computational prediction of flow-generated sound. *Annu. Rev. Fluid Mech.* **2015**, *38*, 483–512. [CrossRef]
19. Liu, H.L.; Dai, H.W.; Ding, J.; Tan, M.G.; Wang, Y.; Huang, H.Q. Numerical and experimental studies of hydraulic noise induced by surface dipole sources in a centrifugal pump. *J. Hydrodyn.* **2016**, *28*, 43–51. [CrossRef]
20. Langthjem, M.A.; Olhoff, N. A numerical study of flow-induced noise in a two-dimensional centrifugal pump. Part I. Hydrodynamics. *J. Fluid Struct.* **2004**, *19*, 349–368. [CrossRef]
21. Langthjem, M.A.; Olhoff, N. A numerical study of flow-induced noise in a two-dimensional centrifugal pump. Part II. Hydroacoustics. *J. Fluid Struct.* **2004**, *19*, 36–386. [CrossRef]
22. Huang, J.X.; Geng, S.J.; Wu, R.; Liu, K.; Nie, C.Q.; Zhang, H.W. Comparison of noise characteristics in centrifugal pumps with different types of impellers. *Acta Acoust.* **2010**, *35*, 113–118.
23. Ma, Z.L.; Chen, E.Y.; Guo, Y.L.; Yang, A.L. Numerical Simulation of the Influence of the Diameter at the Outlet of an Impeller on the Noise Level Induced by the Flow Inside a Centrifugal Pump. *J. Eng. Therm. Energy Power* **2016**, *31*, 93–98.
24. Liu, H.L.; Ding, J.; Tan, M.G.; Cui, J.B.; Wang, Y. Analysis and experimental of centrifugal pump noise based on outlet width of impeller. *Trans. Chin. Soc. Agric. Eng.* **2013**, *29*, 66–73.
25. Gao, M.; Dong, P.X.; Lei, S.H.; Turan, A. Computational Study of the Noise Radiation in a Centrifugal Pump When Flow Rate Changes. *Energies* **2017**, *10*, 221. [CrossRef]

26.　Dong, P.X.; Gao, M.; Guan, H.J.; Lu, D.Y.; Song, K.Q.; Sun, F.Z. Numerical simulation for variation law of volute radiated noise in centrifugal pumps under variable rotating speed. *J. Vib. Shock* **2017**, *36*, 128–133.

27.　Tao, J.Y.; Lu, X.N.; Wang, L.L. *Methods of Measuring and Evaluating Noise of Pumps*; Chinese Quality Supervision Bureau: Beijing, China, 2013.

28.　Du, G.H.; Zhu, Z.M.; Gong, X.F. *Fundamentals of Acoustics*; Nanjing University Press: Nanjing, China, 2001.

29.　Dong, P.X. Computational Study on the Noise Radiation of a Centrifugal Pump Based on 3-D Flow field with Varying Working Condition. Master's Thesis, Shandong University, Jinan, China, 2016.